Numerical computation of the beta function of large N SU(N) gauge theory coupled to an adjoint Dirac fermion

A. Hietanen and R. Narayanan

Numerical computation of the beta function of large N SU(N) gauge theory coupled to an adjoint Dirac fermion

A. Hietanen[*]

CP3-Origins and the Danish Institute for Advanced Study DIAS,
University of Southern Denmark, Campusvej 55, DK-5230 Odense M, Denmark.

R. Narayanan[†]

Department of Physics, Florida International University, Miami, FL 33199, USA.

We use a single site lattice in four dimensions to study the scaling of large N Yang-Mills field coupled to a single massless Dirac fermion in the adjoint representation. We use the location of the strong to weak coupling transition defined through the eigenvalues of the folded Wilson loop operator to set a scale. We do not observe perturbative scaling in the region studied in this paper. Instead, we observe that the scale changes very slowly with the bare coupling. The lowest eigenvalue of the overlap Dirac operator is another scale that shows similar behavior as a function of the lattice coupling.

I. INTRODUCTION

Particle accelerators experiments provide strict bounds for the beyond standard model physics. For technicolor it means that the coupling constant has to exhibit walking behavior. Otherwise the theory cannot simultaneously explain the mass pattern of standard model fermions and the suppression of the flavor changing neutral currents [1–4]. Hence, lattice studies of vector like gauge theories with appropriate choice of fermion matter with the aim of understanding the conformal window has recently attracted considerable attention(see [5] and references therein). The gauge group is chosen to be SU(N) and the number and representation of fermions is such that the theory is expected to be conformal or near conformal [6].

Let

$$b = \frac{1}{g^2 N} \tag{1}$$

define the inverse 't Hooft coupling on the lattice. Let

$$t = \ln a \tag{2}$$

define the logarithm of a lattice scale where $a(b)$ could be the square root of the string tension measured on the lattice at the coupling b. The beta function of the lattice is defined as

$$\beta(b) = \frac{db(t)}{dt}. \tag{3}$$

The perturbative beta function leads off as

$$\beta(b) = -b_0 - \frac{b_1}{b} + \cdots. \tag{4}$$

As is well known [7], only the one and two loop coefficients, b_0 and b_1, are universal and the higher order coefficients in a Taylor expansion of $\beta(b)$ in powers of b^{-1} depend on the choice of $a(b)$. In fact, one can imagine choosing an $a(b)$ such that all higher order coefficients are zero. We will not have such control on the choice of $a(b)$. In particular,

———

[*]Electronic address: `hietanen@cp3-origins.net`
[†]Electronic address: `rajamani.narayanan@fiu.edu`

there is no reason to expect the location of the zero of the beta function to be independent of the choice of $a(b)$ – all we can expect is for the zero to remain stable if it is at a perturbatively weak coupling.

The choice of fermionic matter can be motivated by the presence of a zero in the two-loop perturbative beta function. In order to maintain asymptotic freedom, all choices are such that $b_0 > 0$. The two loop beta function has a zero if $b_1 < 0$. Some of the choices currently being investigated are:

- SU(3) gauge group with twelve Dirac flavors of fermions in the fundamental representation [8–10] – b_1 is negative if we have nine or more Dirac flavors but the zero of the two loop beta function occurs at smaller coupling for larger flavors.

- SU(2) gauge group with two Dirac flavors of fermions in the adjoint representation [11–14] – This is the only choice based upon b_0 and b_1 since $b_0 < 0$ if we choose three or more Dirac flavors and $b_1 > 0$ if we choose one Dirac flavor.

- SU(3) gauge group with two Dirac flavors in the two-index symmetric representation [15–17] – In this case $b_1 > 0$ if there is only one Dirac flavor. One can also choose three Dirac flavors and still maintain asymptotic freedom.

The case of SU(N) gauge theory coupled to f flavors of Dirac fermions in the adjoint representation is interesting for two reasons:

- The first two coefficients of the beta function are

$$b_0 = \frac{11 - 4f}{24\pi^2}; \quad b_1 = \frac{17 - 16f}{192\pi^4},$$ (5)

  and are independent of N [33]. The three interesting choices for a theory with an infra-red fixed point are $f = \frac{3}{2}, 2, \frac{5}{2}$ based on the two-loop beta function.

- Numerical evidence along with continuum arguments [18]-[26] suggest that Eguchi-Kawai reduction holds in the large N limit as long as one uses periodic boundary conditions for fermions. This is expected to be the case for $f \geq \frac{1}{2}$ [22] and for non-zero quark masses [19].

We have the possibility to study theories with an infra-red fixed point that have only four $SU(N)$ degrees of freedom provided we consider the $N \to \infty$ limit. For finite N, the massless fermionic operator is a finite dimensional operator that decouples into chiral sectors. The fermion determinant is positive in each chiral sector and we can define a theory for any real value f since we can write

$$(\det \not{D})^f = e^{f \ln \det \not{D}}.$$ (6)

If $\frac{11}{4} > f > \frac{17}{16}$, the two loop beta function has a zero and the theory has an infra-red fixed point.

Our aim in this paper is to use overlap fermions [28]-[30] and study the $f = 1$ theory on a single site lattice. We do not expect the beta function to have a zero from the perturbative viewpoint. Even if it has a zero, we expect it to be at strong coupling. With this in mind we expect a computation of the running coupling to agree with the two-loop running. Contrary to this expectation, we will show that the coupling runs much faster than what is expected from perturbative running.

The model on the single site lattice is defined in Sec. II. We will numerically study this model using the Hybrid Monte Carlo (HMC) algorithm with pseudofermions as described in Sec. III. It is numerically difficult to extract the string tension. On the other hand there is an observable based on the Wilson loop operator [31, 32] that shows a transition from weak to strong coupling and we will use the location of this transition to set our scale as discussed in Sec. IV A. We will also look at the eigenvalues closest to zero of the overlap Dirac operator. We will compare the behavior of the lowest positive eigenvalue as a function of the lattice coupling and compare its behavior to the scale set using the Wilson loop operator.

Results for the behavior of the scales set using the Wilson loop operator and the lowest positive eigenvalue of the massless Dirac operator are discussed in detail for the case of theory with massless fermions in Sec. V. We will show that both scales are monotonic in the coupling and that they both vary very slowly with the coupling.

II.   THE MODEL

The action on a single site lattice with one flavor of adjoint Dirac overlap fermion is given by

$$S = S_g + S_f.$$ (7)

The gauge action is

$$S_g = -12bNP; \quad P = \frac{1}{12} \sum_{\mu \neq \nu = 1}^{4} \mathrm{Tr} \left[U_\mu U_\nu U_\mu^\dagger U_\nu^\dagger \right], \tag{8}$$

where the four gauge degrees of freedom, U_μ ($\mu = 1, 2, 3, 4$), are SU(N) matrices. The lattice gauge coupling constant is $b = \frac{1}{g^2 N}$. The overlap fermion action is

$$S_f = -f \ln \det H_o(\mu), \tag{9}$$

where the Hermitian massive overlap Dirac operator is defined by

$$H_o(\mu) = \frac{1}{2} \left[(1 + \mu) \gamma_5 + (1 - \mu) \epsilon(H) \right], \tag{10}$$

with $\mu \in [0, 1]$ being the bare mass. We note that the eigenvalues of $H_o(0)$ are in the range $[-1, 1]$ with exact zero eigenvalues and exact ± 1 eigenvalues corresponding to a gauge background with non-zero topology. The Hermitian Wilson Dirac operator for adjoint fermions is given by

$$\begin{aligned} H &= \begin{pmatrix} 4 - m - \frac{1}{2} \sum_\mu \left(V_\mu + V_\mu^t \right) & \frac{1}{2} \sum_\mu \sigma_\mu \left(V_\mu - V_\mu^t \right) \\ -\frac{1}{2} \sum_\mu \sigma_\mu^\dagger \left(V_\mu - V_\mu^t \right) & -4 + m + \frac{1}{2} \sum_\mu \left(V_\mu + V_\mu^t \right) \end{pmatrix} \\ &= (4 - m)\gamma_5 - \sum_\mu \left(w_\mu V_\mu + w_\mu^\dagger V_\mu^t \right), \end{aligned} \tag{11}$$

where

$$w_\mu = \frac{1}{2} \begin{pmatrix} 1 & -\sigma_\mu \\ \sigma_\mu^\dagger & -1 \end{pmatrix} \tag{12}$$

and V_μ are the link matrices in adjoint representation. The action of V_μ on Φ is given by

$$V_\mu \Phi = U_\mu \Phi U_\mu^\dagger; \quad V_\mu^t \Phi = U_\mu^\dagger \Phi U_\mu. \tag{13}$$

One can verify that H is Hermitian in the usual sense:

$$\mathrm{Tr} \Psi^\dagger H \Phi = \left[\mathrm{Tr} \Phi^\dagger H \Psi \right]^* = \mathrm{Tr} \left[(H\Psi)^\dagger \Phi \right]. \tag{14}$$

Therefore $\Psi^\dagger H = (H\Psi)^\dagger$ and in addition it is also true that $\mathrm{Tr} H\Phi = 0$ if $\mathrm{Tr}\Phi = 0$. The same is also true for $H_o(\mu)$.

III. THE NUMERICAL ALGORITHM

We used the Hybrid Monte Carlo (HMC) algorithm to generate U_μ according to the measure

$$Z = \int [dU_\mu] e^{-S}. \tag{15}$$

Let us introduce a Hamiltonian

$$\mathcal{H} = \frac{1}{2} \sum_{\mu=1}^{4} \mathrm{Tr} H_\mu^2 + S, \tag{16}$$

where matrices, H_μ; $\mu = 1, 2, 3, 4$ are elements of the $su(N)$ algebra and conjugate to U_μ. The HMC algorithm involves the computation of the force, $\frac{\partial S}{\partial U_\mu^{ij}}$. The gauge part of the force is simple to compute numerically, but the fermionic part of the force is computationally intensive. An *exact* algorithm was developed in [22] to compute the fermionic part of the force. This algorithm scales like N^6. In addition to using this algorithm, we also developed a pseudo-fermion algorithm in order to compute the fermionic part of the force which scales like N^4. We present the details of the pseudo-fermion algorithm in this section. Both algorithms were used to obtain the numerical data presented in this paper.

We note that

$$H_{o\pm}^2(\mu) = \frac{1+\mu^2}{2}P_\pm \pm \frac{1-\mu^2}{2}P_\pm\epsilon(H)P_\pm; \quad P_\pm = \frac{1\pm\gamma_5}{2}, \tag{17}$$

and

$$\det H_o(\mu) = \det H_{o+}^2(\mu) = \det H_{o-}^2(\mu), \tag{18}$$

in the zero topological sector. [34] The overlap fermion action can be rewritten as

$$S_f = \mathrm{Tr}\left[\Phi_+^\dagger \left[H_{o+}^2(\mu)\right]^{-1}\Phi_+\right]; \tag{19}$$

where the pseudofermions Φ_+ have positive chirality and are traceless $N \times N$ complex matrices with an additional two component spin index.

For numerical purposes, we will represent $\epsilon(H)$ as

$$\epsilon(H) = \sum_{k=1}^n \frac{r_k H}{H^2 + p_k}; \quad 0 < p_1 < p_2 \cdots < p_n, \tag{20}$$

with n chosen such that the representation is accurate in the spectral range of H^2 assuming some lower bound on the spectrum of H^2.

The algorithm starts with one choice for U_μ. Then, we draw H_μ according to a Gaussian distribution. We also draw Dirac indexed traceless Hermitian matrices, Ψ according to the Gaussian distribution, $\mathrm{Tr}\Psi^\dagger\Psi$, and set

$$\Phi_+ = P_+ H_o(\mu)\Psi. \tag{21}$$

The equations of motion for U_μ are

$$\frac{dU_\mu}{d\tau} = iH_\mu U_\mu. \tag{22}$$

Setting $\frac{d\mathcal{H}}{d\tau} = 0$ results in

$$\sum_{\mu=1}^4 \mathrm{Tr}\left[H_\mu \frac{dH_\mu}{d\tau}\right] + \frac{dS_g}{d\tau} + \frac{dS_f}{d\tau} = 0, \tag{23}$$

and

$$\frac{dS_g}{d\tau} = \sum_{\mu=1}^4 \mathrm{Tr}\left[H_\mu D_\mu^g\right]; \quad \frac{dS_f}{d\tau} = \sum_{\mu=1}^4 \mathrm{Tr}\left[H_\mu D_\mu^f\right]. \tag{24}$$

The equation of motion for H_μ is given by

$$\frac{dH_\mu}{d\tau} = -D_\mu^g - D_\mu^f. \tag{25}$$

Taking the derivative of S_g in (8) with respect to τ and using (22) we arrive at

$$D_\mu^g = -ibN \sum_{\nu=1}^4 \left[U_\mu U_\nu U_\mu^\dagger U_\nu^\dagger + U_\mu U_\nu^\dagger U_\mu^\dagger U_\nu - U_\nu^\dagger U_\mu U_\nu U_\mu^\dagger - U_\nu U_\mu U_\nu^\dagger U_\mu^\dagger\right] \tag{26}$$

The derivative of S_f in (19) with respect to τ using (17) is

$$\frac{dS_f}{d\tau} = -\frac{1-\mu^2}{2}\mathrm{Tr}\left[\Upsilon_+^\dagger \frac{d\epsilon(H)}{d\tau}\Upsilon_+\right]; \quad \Upsilon_+ = \left[H_{o+}^2(\mu)\right]^{-1}\Phi_+. \tag{27}$$

Substituting the representation (20) for $\epsilon(H)$, we can write

$$\frac{dS_f}{d\tau} = -\frac{1-\mu^2}{2}\sum_{k=1}^n \left(r_k p_k \mathrm{Tr}\left[\Upsilon_k^\dagger \frac{dH}{d\tau}\Upsilon_k\right] - r_k \mathrm{Tr}\left[\Xi_k^\dagger \frac{dH}{d\tau}\Xi_k\right]\right); \tag{28}$$

where

$$\Upsilon_k = \frac{1}{H^2 + p_k}\Upsilon_+; \quad \Xi_k = H\Upsilon_k. \tag{29}$$

Using (11), (13) and (22), we can show that

$$\mathrm{Tr}\left[X^\dagger \frac{dH}{d\tau}X\right] = \sum_{\mu=1}^{4}\mathrm{Tr}\left[H_\mu A_\mu(X)\right], \tag{30}$$

where

$$A_\mu(X) = i\sum_{i,j=1}^{4}\left(w_\mu^{\dagger\, ij}\left[X_j, U_\mu X_i^\dagger U_\mu^\dagger\right] + w_\mu^{\,ij}\left[X_i^\dagger, U_\mu X_j U_\mu^\dagger\right]\right), \tag{31}$$

for any complex matrix X. It is clear that $A_\mu^\dagger(X) = A_\mu(X)$ and that $\mathrm{Tr}A_\mu(X) = 0$. Therefore,

$$D_\mu^f = -\frac{1-\mu^2}{2}\sum_{k=1}^{n}\left[r_k p_k A_\mu(\Upsilon_k) - r_k A_\mu(\Xi_k)\right]. \tag{32}$$

Given Φ_+ in (21), we compute Υ_+ in (27) with the standard conjugate gradient algorithm. Each action of $H_{o+}^2(\mu)$ that is part of the conjugate gradient algorithm involves the action of $\epsilon(H)$ on a Dirac indexed traceless Hermitian matrix. We use the multiple mass conjugate algorithm for each action of $\epsilon(H)$ represented by (20). The core of the fermion algorithm is the action of H on a Dirac indexed traceless Hermitian matrix and this operation scales like N^3 [see (13)]. In addition, the computational cost depends on the gap of H and $H_{o+}(\mu)$. The former is large and therefore does not seriously affect the computational cost. Since we are interested in studying chiral properties of the theory and want to work with as small a bare mass, μ, as possible the smallest eigenvalues of $H_{o+}(0)$ will scale like N^{-2} and the condition number grows like N^2.

IV. OPERATORS

We will focus on measuring two quantities that will help us understand the running of the coupling with the scale and reveal numerical evidence for a singular point. One observable looks at the property of the gauge field and the other looks at the property of the massless fermion.

A. Weak to strong coupling transition [32]

A folded $L \times L$ square Wilson loop operator in the $\mu - \nu$ plane is given by

$$W(L) = U_\mu^L U_\nu^L U_\mu^{\dagger\, L} U_\nu^{\dagger\, L}. \tag{33}$$

The eigenvalues, $e^{i\theta_k};\ k = 1, \cdots, N$ of this operator are gauge invariant. Let $p(\theta; L, b)$ be the distribution of these eigenvalues with $\theta \in [-\pi, \pi)$. This distribution undergoes a transition at $N \to \infty$ as the size, L, is changed at a fixed coupling b: the distribution has a gap at π for small areas and it becomes gapless for areas larger than a critical area $A_c(b)$. There is a universal function describing the distribution in terms of the scaled variables derived from $A(b)$ and θ in the vicinity of $A_c(b)$ and π.

Let

$$O_N(y; L, b) = \left\langle \det\left(e^{\frac{y}{2}} + e^{-\frac{y}{2}}W(L)\right)\right\rangle. \tag{34}$$

The region close to $y = 0$ probes θ close to π. Let

$$O_N(y; L, b) = C_0(L, b, N) + C_1(L, b, N)y^2 + C_2(L, b, N)y^4 + \cdots. \tag{35}$$

It is useful to define a Binder cumulant type quantity

$$\Omega(L, b, N) = \frac{C_0(L, b, N)C_2(L, b, N)}{C_1^2(L, b, N)}. \tag{36}$$

One can show using the universal scaling function that

$$\Omega(L_c(b), b, \infty) = \frac{\Gamma^4\left(\frac{1}{4}\right)}{48\pi^2} = 0.364739936 \tag{37}$$

We can define $L_c(b, N)$ at a fixed N and b as the length where

$$\Omega(L_c(b, N), b, N) = 0.364739936, \tag{38}$$

and

$$\lim_{N \to \infty} L_c(b, N) = L_c(b), \tag{39}$$

will be the location of the transition at infinite N.

Since we are working at a fixed but large N in this paper, we will define our length scale as

$$a(b) = \frac{1}{L_c(b, N)}. \tag{40}$$

B.   Low lying fermion eigenvalues

The eigenvalues of the massless Hermitian overlap Dirac operator, $H_o(0)$, can be used to see how they scale and if they show evidence for chiral symmetry breaking. The eigenvalues come in doubly degenerate pairs and there is also a pairing of positive and negative eigenvalues due to exact chiral symmetry on the lattice. We computed all the eigenvalues of the massless overlap Dirac operator.

Let $0 < \lambda_k < 1$, $k = 1, \cdots, N^2 - 1$ with $\lambda_k < \lambda_{k+1}$ denote all the positive distinct eigenvalues where each eigenvalue is doubly degenerate and each positive eigenvalue has a negative eigenvalue pair. We can use

$$\lambda(b) = \langle \lambda_1 \rangle \tag{41}$$

as another choice for our length scale.

If chiral symmetry is broken, the chiral condensate sets a scale. In particular, we expect

$$r_k = \left\langle \frac{\lambda_1}{\lambda_k} \right\rangle \tag{42}$$

to be independent of the coupling for a few low values of k. As N increases, we expect more r_k to be independent of the coupling. In addition, we expect $\lambda(b)$ to approach a finite limit as $N \to \infty$.

V.   SINGLE SITE MODEL WITH MASSLESS ADJOINT FERMIONS

Our choice of b and N are based on numerical feasibility. We expect the approach to the large N limit to get slower as we increase b. Since the numerical costs increase rapidly with N, we cannot make N as large as we wish. Computational costs are manageable if we choose N in the range of 13 to 25. We will restrict ourselves to a single value of N, namely, $N = 18$. We have chosen the couplings in the range $b \in [0.32, 0.70]$. Our definition of the coupling is related to the conventional lattice coupling by

$$\beta = 2bN^2. \tag{43}$$

Our range of coupling corresponds to $\beta \in [2.56, 5.6]$ for SU(2) and $\beta \in [5.76, 12.6]$ for SU(3). The choice of couplings falls in the range of recent simulations with adjoint fermions using SU(2) as the gauge group [11–13] and also in simulations with fermions in the symmetric two-index representation and SU(3) as the gauge group [15].

In addition to these physical parameters, we also have to choose the value of the Wilson mass parameter, m, in (11). It is an irrelevant parameter but needs to be chosen in a specific range to realize the correct continuum limit. Based on previous studies on a single site model with adjoint fermions [19], we set $m = 4$ in this paper.

Table I shows the various values of couplings where simulations were performed along with the results for the average plaquette (c.f. (8)), $a(b)$ (c.f. (40)), and $\lambda(b)$ (c.f. 41)). A plot of the average plaquette is shown in Fig. 1. The plaquette leads off as $1 - \frac{N-1}{8Nb} + O(b^{-2})$ where the coefficient of b^{-1} is not affected by fermions. A fit of the

b	$\langle P \rangle$	$a(b)$	$\lambda(b)$
0.32	0.6092(7)	0.4442(24)	0.9766(136)
0.35	0.6290(7)	0.4251(23)	0.9102(119)
0.40	0.6720(7)	0.3858(22)	0.7889(102)
0.45	0.7045(6)	0.3561(29)	0.6841(87)
0.50	0.7325(5)	0.3354(27)	0.5925(77)
0.53	0.7468(5)	0.3050(36)	0.5400(73)
0.55	0.7562(5)	0.2931(29)	0.5003(73)
0.57	0.7650(5)	0.2820(28)	0.4986(69)
0.60	0.7775(5)	0.2704(26)	0.4602(70)
0.65	0.7943(5)	0.2566(29)	0.4114(61)
0.70	0.8076(4)	0.2354(131)	0.3823(54)

TABLE I: Table showing the various values of couplings where simulations were performed with massless fermions with $N = 18$. The results for the average plaquette and the two different choices for the scales are also shown.
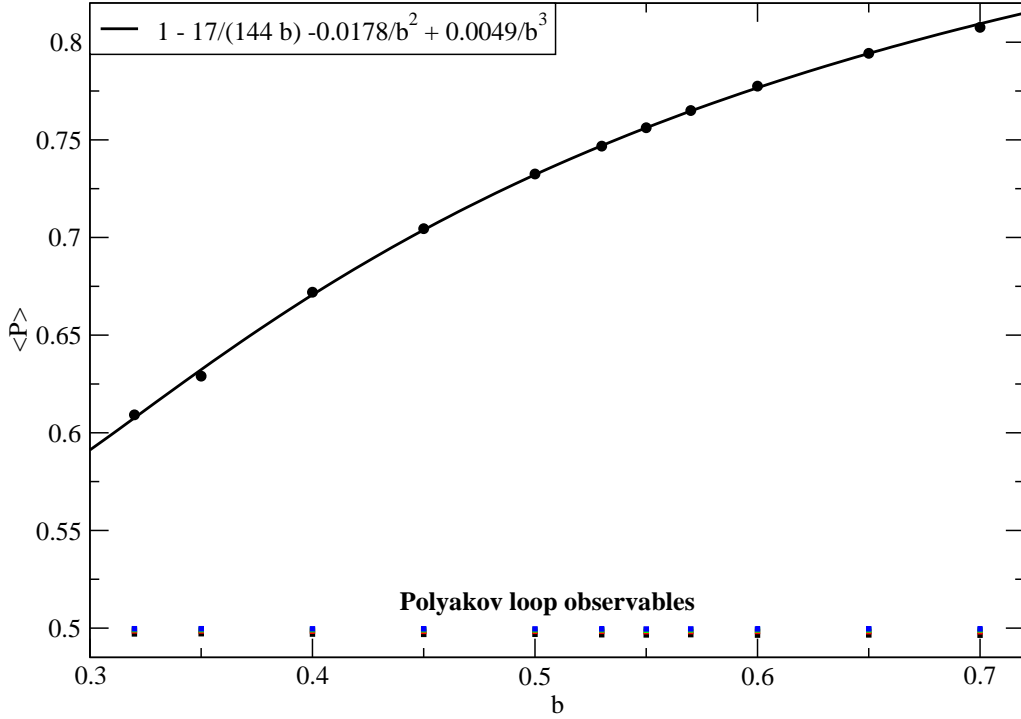
FIG. 1: Average value of the plaquette along with the average values for the four different Polyakov loop observables for massless fermions at $N = 18$.

data shows a smooth approach to unity as $b \to \infty$. The data also shows a measure of the fact that the eigenvalues of Polyakov loop operators U_μ are uniformly distributed. The four data points shown by different colored squares, correspond to the average values of

$$P_\mu = \frac{1}{2} \left(1 - \frac{1}{N^2} |\mathrm{Tr} U_\mu|^2 \right) ; \tag{44}$$

for $\mu = 1, \cdots, 4$ with $P_1 < P_2 < P_3 < P_4$ on every gauge field configuration. An average value of $\frac{1}{2}$ in the large N limit shows that the Z_N symmetries are not broken. Our results are very close to $\frac{1}{2}$ and we can assume that reduction to a single site holds and we are simulating an infinite volume theory.

We define

$$b_{\text{tad}} = b\langle P \rangle, \tag{45}$$

as the tadpole improved coupling and plot the running of this coupling versus our two logarithmic scales, $\ln a(b)$ and $\ln \lambda(b)$ in Fig. 2 and Fig. 3 respectively for the data points listed in Table I. The data with errorbars are shown with solid circles in both figures. We chose one point in the middle of the range as our renormalization point and the solid curve represents the result based on two loop perturbation theory. Clearly, there is no agreement and the coupling runs much faster than what is expected from two loop perturbation theory. This indicates that we are working with lattice couplings that should be considered as strong in spite of the fact that we used values that would be considered as weak in theories that do not have additional fixed points.
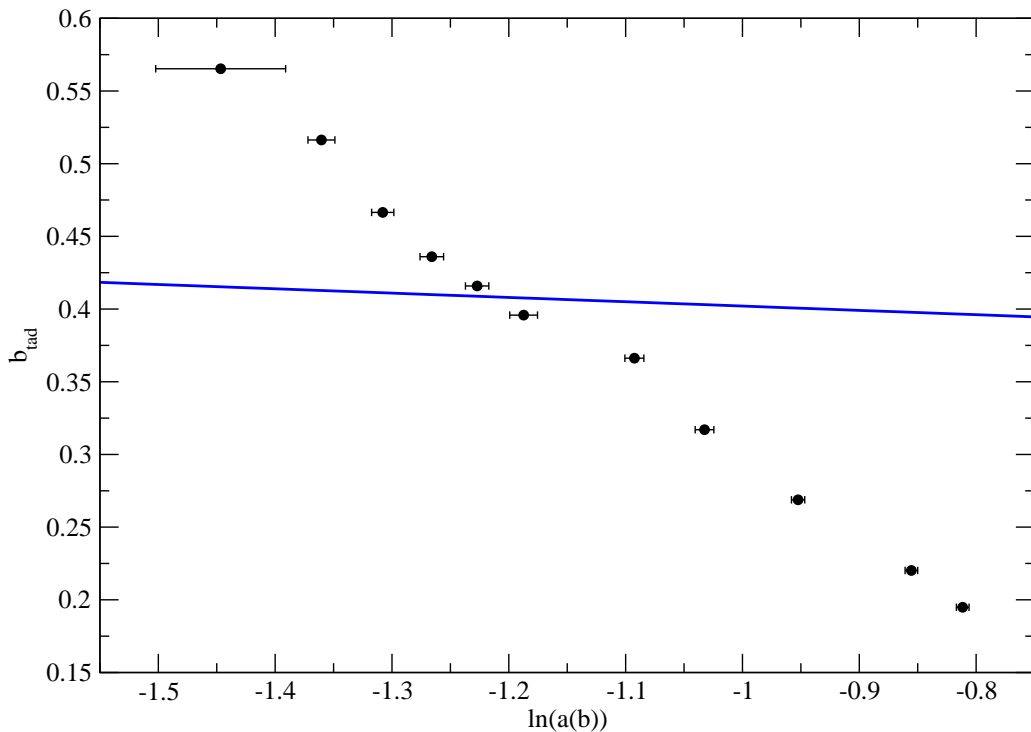

FIG. 2: Running of the tadpole improved coupling versus the logarithmic scale $\ln a(b)$ for massless fermions at $N = 18$.

We end this section by presenting some details pertaining to the two scales. We start by noting that L does not have to be an integer in (33). We can always write

$$U_\mu = g_\mu e^{i\Theta_\mu} g_\mu^\dagger, \tag{46}$$

where g_μ is the unitary matrix that diagonalizes U_μ and Θ_μ is diagonal with all entries in the range $(-\pi, \pi]$. Then, we can write

$$U_\mu^L = g_\mu e^{iL\Theta_\mu} g_\mu^\dagger, \tag{47}$$

for any real value, L. Assuming that this is done on every configuration, we can compute $\Omega(L, N, b)$ in (36) as a continuous function of L. Fig. 4 shows such a plot at $N = 18$ and $b = 0.55$. The oscillations we see in that plot is a
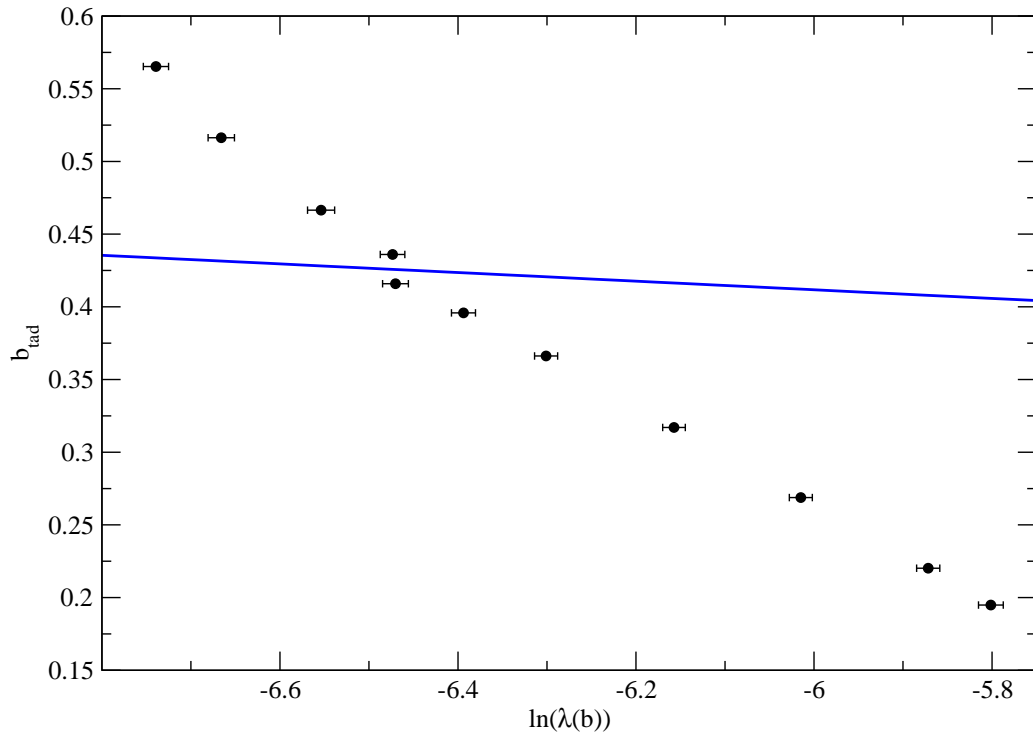
FIG. 3: Running of the tadpole improved coupling versus the logarithmic scale $\ln \lambda(b)$ for massless fermions at $N = 18$.

finite N effect. The red point in that figure is an estimate of $a(b)$ defined through (38) and (40) and listed in Table I. The numbers in Table I were obtained only using integer values of L and a linear interpolation between the integer values.

Fig. 5 is a plot of the eigenvalues of the Wilson loop operator at $N = 18$ and $b = 0.32$ for three different values of L, namely, $\frac{1}{a(b)}$, $\frac{3}{a(b)}$ and $\frac{1}{3a(b)}$ with $a(b)$ set according to the value in Table I for $b = 0.32$. Clearly, the eigenvalues close to π die down exponentially for the smallest loop and the eigenvalues fill the full range for the largest loop. The critical loop shows a distribution that just covers the entire range.

The complete spectrum of the distinct eigenvalues of the massless adjoint overlap Dirac operator are shown in Fig. 6 for three different couplings. All three plots show the same qualitative behavior. We see a concentration of small eigenvalues (less than 0.1) followed by a bulk like distribution. We think the distribution for $\lambda < 0.1$ is due to the would be zero modes in the gauge field background that is diagonal. We believe that this part of the distribution will shows signs of chiral symmetry breaking if one exists.

The plot of r_k as defined in (42) versus k is shown in a log-log plot in Fig. 7. Here again, one sees a separation between the low eigenvalues (the would-be zero modes in a diagonal background) and the bulk. Furthermore, the ratios do not change much with coupling for $k < 5$ and we expect this range to increase as we go to larger N. This is in agreement with chiral symmetry being broken in this theory.

VI. CONCLUSIONS

The single site model of a large N gauge theory coupled to massless adjoint fermions was numerically studied in this paper. We have studied this model with a single flavor of adjoint fermion numerically using the Hybrid Monte Carlo algorithm and pseudofermions. We studied the running coupling using two different choice of scales and did not
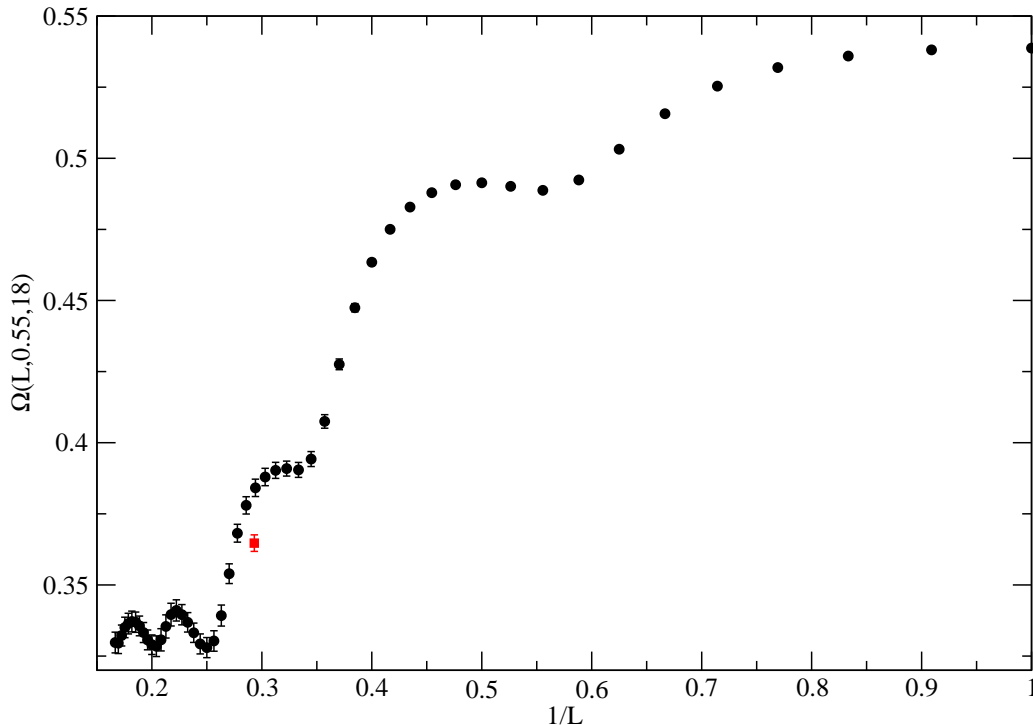
FIG. 4: Plot of the quantity, $\Omega(L, N, b)$, as a function of L^{-1} at $N = 18$ and $b = 0.55$ for massless fermions. The red square is the estimate listed in Table I.

find agreement with two-loop perturbation theory at intermediate values of the tadpole improved coupling. The two different choices of scales were the transition from weak to strong coupling and the lowest eigenvalue of the massless overlap Dirac operator. This is the main result of our paper.

Both Fig. 2 and Fig. 3 show a mild discontinuity at a certain value of the tadpole improved coupling that is close to 0.4. This might be a lattice artifact but it could also signal some non-trivial behavior in the beta function that is prohibiting an approach to a perturbative scaling behavior at the values of the coupling studied in this paper. The results presented in this paper are exploratory in nature and future simulations with different values of f will give a clearer physics picture. However, the work lays the foundation for the careful study of ultra-violet/infra-red fixed points in matrix models that mimic large N gauge theories coupled to adjoint fermions. We have the ability to treat the number of fermion flavors as a real number in the matrix model and study the presence of singular behavior in the associated beta function. It is likely that the behavior at the singular point, results in it being an ultra-violet/infra-red fixed point for some range of fermion flavors. The numerical procedure developed in this paper for the case of a single Dirac flavor paves the way for future numerical studies of the matrix model with varying number of flavors.
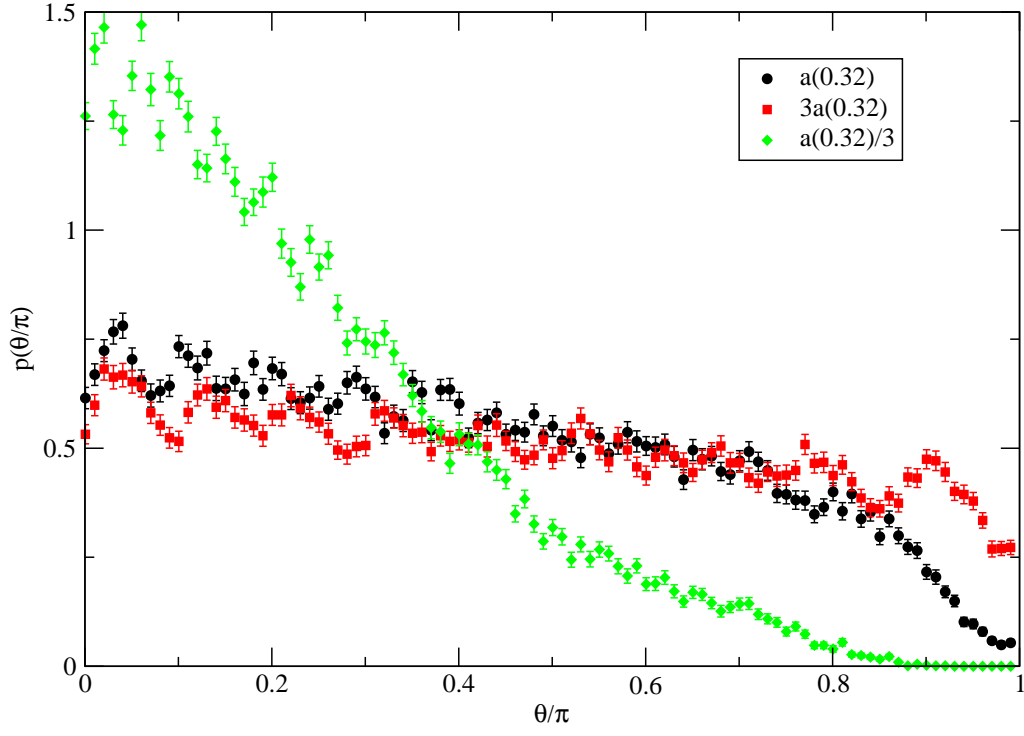
Acknowledgments

FIG. 5: The distribution of the eigenvalues of the square Wilson loop operators for three different sizes at $N = 18$ and $b = 0.32$ with massless fermions.
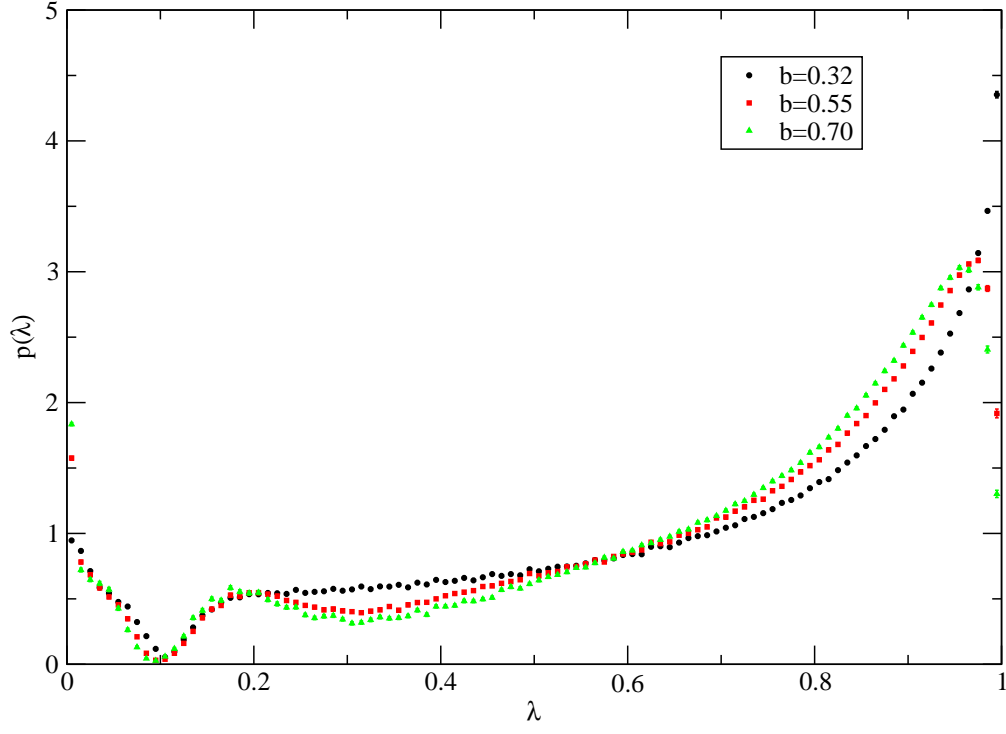
FIG. 6: The full distribution of the eigenvalues of the massless adjoint overlap Dirac operator for three different couplings at $N = 18$.
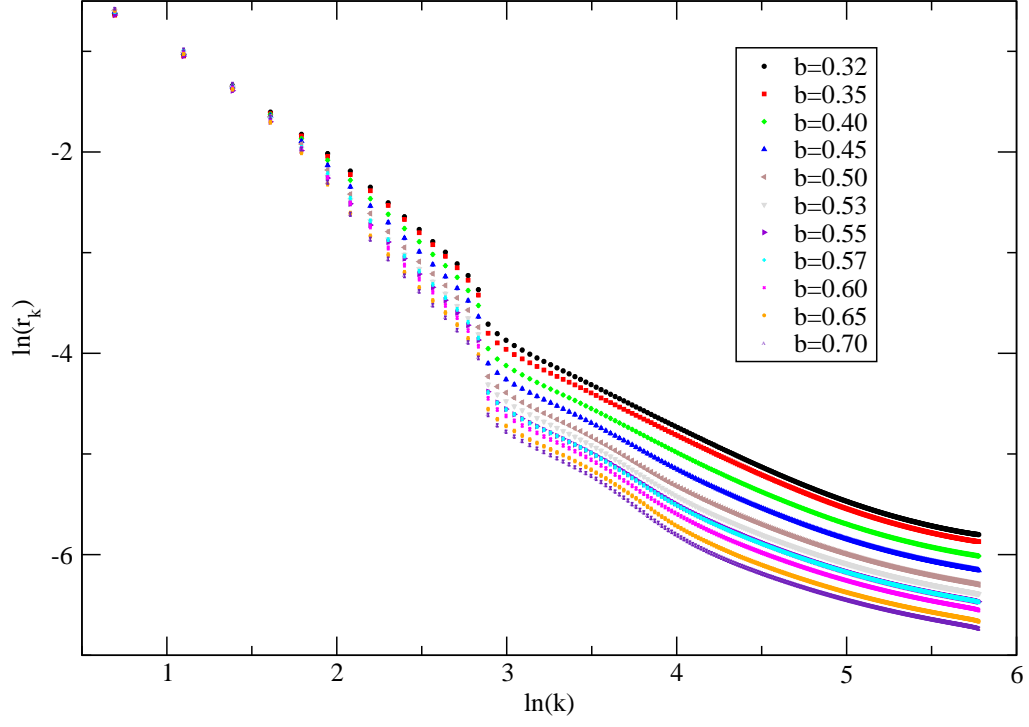
FIG. 7: The ratios of the eigenvalues of the massless adjoint overlap Dirac operator are shown in log-log plot for all the data listed in Table I.

[1] B. Holdom, Phys. Rev. D **24**, 1441 (1981).
[2] K. Yamawaki, M. Bando and K. -i. Matumoto, Phys. Rev. Lett. **56**, 1335 (1986).
[3] T. W. Appelquist, D. Karabali and L. C. R. Wijewardhana, Phys. Rev. Lett. **57**, 957 (1986).
[4] J. R. Andersen, O. Antipin, G. Azuelos, L. Del Debbio, E. Del Nobile, S. Di Chiara, T. Hapola, M. Jarvinen *et al.*, [arXiv:1104.1255 [hep-ph]].
[5] L. Del Debbio, PoS **LATTICE2010**, 004 (2010).
[6] F. Sannino and K. Tuominen, Phys. Rev. D **71**, 051901 (2005) [hep-ph/0405209]. D. D. Dietrich, F. Sannino, Phys. Rev. **D75**, 085018 (2007). [hep-ph/0611341].
[7] S. Weinberg, Cambridge, UK: Univ. Pr. (1996) 489 p
[8] A. Hasenfratz, [arXiv:1106.5293 [hep-lat]].
[9] T. Appelquist, G. T. Fleming, M. Lin, E. T. Neil, D. A. Schaich, [arXiv:1106.2148 [hep-lat]].
[10] Z. Fodor, K. Holland, J. Kuti, D. Nogradi, C. Schroeder, Phys. Lett. **B703**, 348-358 (2011). [arXiv:1104.3124 [hep-lat]].
[11] S. Catterall, L. Del Debbio, J. Giedt, L. Keegan, [arXiv:1108.3794 [hep-ph]].
[12] T. DeGrand, Y. Shamir, B. Svetitsky, Phys. Rev. **D83**, 074507 (2011). [arXiv:1102.2843 [hep-lat]].
[13] A. J. Hietanen, K. Rummukainen, K. Tuominen, Phys. Rev. **D80**, 094504 (2009). [arXiv:0904.0864 [hep-lat]].
[14] F. Bursa, L. Del Debbio, D. Henty, E. Kerrane, B. Lucini, A. Patella, C. Pica and T. Pickup *et al.*, Phys. Rev. D **84**, 034506 (2011) [arXiv:1104.4301 [hep-lat]].
[15] Y. Shamir, B. Svetitsky, T. DeGrand, Phys. Rev. **D78**, 031502 (2008). [arXiv:0803.1707 [hep-lat]].
[16] Z. Fodor, K. Holland, J. Kuti, D. Nogradi, C. Schroeder, [arXiv:1103.5998 [hep-lat]].
[17] J. B. Kogut, D. K. Sinclair, [arXiv:1105.3749 [hep-lat]].
[18] B. Bringoltz, M. Koren, S. R. Sharpe, [arXiv:1106.5538 [hep-lat]].
[19] A. Hietanen, R. Narayanan, Phys. Lett. **B698**, 171-174 (2011). [arXiv:1011.2150 [hep-lat]].
[20] S. Catterall, R. Galvez, M. Unsal, JHEP **1008**, 010 (2010). [arXiv:1006.2469 [hep-lat]].
[21] T. Azeyanagi, M. Hanada, M. Unsal, R. Yacoby, Phys. Rev. **D82**, 125013 (2010). [arXiv:1006.0717 [hep-th]].
[22] A. Hietanen, R. Narayanan, JHEP **1001**, 079 (2010). [arXiv:0911.2449 [hep-lat]].
[23] E. Poppitz, M. Unsal, JHEP **1001**, 098 (2010). [arXiv:0911.0358 [hep-th]].
[24] B. Bringoltz, JHEP **0906**, 091 (2009). [arXiv:0905.2406 [hep-lat]].
[25] G. Cossu and M. D'Elia, JHEP **0907**, 048 (2009) [arXiv:0904.1353 [hep-lat]].
[26] P. Kovtun, M. Unsal, L. G. Yaffe, JHEP **0706**, 019 (2007). [hep-th/0702021 [HEP-TH]].
[27] D. B. Kaplan, J. -W. Lee, D. T. Son, M. A. Stephanov, Phys. Rev. **D80**, 125005 (2009). [arXiv:0905.4752 [hep-th]].
[28] R. G. Edwards, U. M. Heller, R. Narayanan, Phys. Rev. **D59**, 094510 (1999). [hep-lat/9811030].
[29] H. Neuberger, Phys. Lett. **B417**, 141-144 (1998). [hep-lat/9707022].
[30] R. Narayanan, H. Neuberger, Nucl. Phys. **B443**, 305-385 (1995). [hep-th/9411108].
[31] R. Narayanan, H. Neuberger, JHEP **0603**, 064 (2006). [hep-th/0601210].
[32] R. Narayanan, H. Neuberger, JHEP **0712**, 066 (2007). [arXiv:0711.4551 [hep-th]].
[33] Trivial coefficients of N get absorbed since we have used the 't Hooft coupling and not g^2.
[34] We are assuming that global topology is completely suppressed and one can restrict the theory to the zero topological sector.